

3-D Amphibious Vehicle Model

1. Summary

As part of the C2M2L modeling effort, we are delivering non-compliant (i.e. “fixed”) terrain profiles that will be used for testing AVM designs. As the terrain profiles are generated in a custom coordinate system, we are providing example vehicle models to illustrate how a typical vehicle is orientated with respect to the terrain model. The specification of the terrain profile is described in Section X, while this appendix illustrates how an amphibious tracked vehicle design can be applied to a set of terrain context models featuring straight, curved, banked and sloped surface sections. The findings suggest that the choice of the coordinate system is crucial to allowing the terrain profiles to be used in a portable way across the surface vehicle standards.

An existing commercial amphibious vehicle, the Hydratrek D2488, was selected to serve as the basis of the vehicle model developed for this task. The current model does not realize the track system on the commercial vehicle, but instead implements a wheeled version. This model interacts with terrain in the form of OpenCRG data files via one of two tire models, a high quality model which uses Pacejka’s “magic formula,” and a fast lower quality model. Both models assume that the ground is rigid.

If the MATLAB Instrument Control Toolbox is available, the example code can be modified¹ so that the example code directly drives the Zulu visualization tool; currently the simulation data is written to a file which can be read by Zulu. It is possible to use the model to drive interactively in Zulu, watching the model react to steering commands in near real time.

The equations of motion developed incorporate a number of approximations designed to speed up the model. There are a number of limitations to the model, and further development is needed to make it truly useful for design work.

1.1 Technical Challenges

The exact equations of motion for a wheeled or tracked vehicle interacting with an uneven compliant terrain are highly nonlinear and extremely complicated. The basic technical challenge in creating a 3-D amphibious vehicle model was to simplify the model enough so that it can run quickly but still retain essential physical authenticity.

1.2 General Methodology

The full equations of motion were derived using no small angle approximations. A MATLAB model was then created which implemented these equations with various approximations

¹ Set the variable DEBUG_VAR_use_udp to true in the file `amphibious_gui.m`.

intended to increase the execution speed of the code. The resulting code was integrated into a simple MATLAB graphical user interface shown in Figure 1.

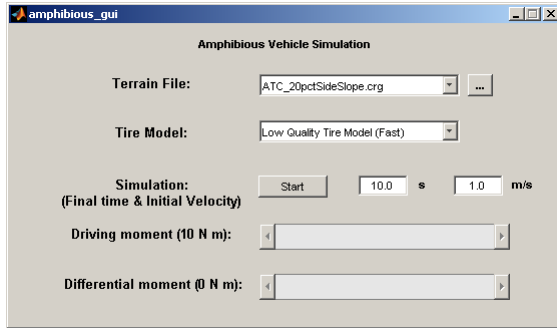


Figure 1. The amphibious vehicle graphical user interface.

The user may select the OpenCRG terrain file and choose which tire model to use from the menus and adjust the final simulation time and the initial velocity before starting the simulation. While the simulation is running the driving and differential moment sliders may be used to interactively drive the vehicle. If the Zulu visualization tool is running and the code has been modified to use it directly (see footnote 1 above), the vehicle will be seen moving in the Zulu window.

1.3 Technical Results

This report documents the development of the equations of motion for an n -axle vehicle, similar to the Hydratrek D2488², but without the over-the-tire rubber track system. (For the vehicle implemented in the example code $n = 4$.) A number of approximations, intended to simplify the analysis, are acknowledged here.

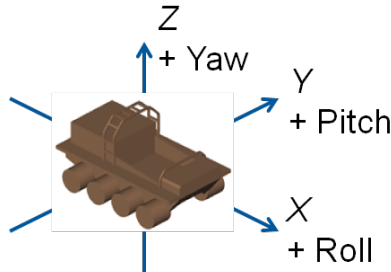


Figure 2. Sign conventions used for developing the equations of motion.

As much as convenient, uppercase vectors are body-fixed, while lowercase vectors are spatial³. Let \mathbf{X} be body-fixed coordinates originating at the center of mass of the vehicle, with X going

² Hydratrek website <<http://www.hydratrek.com/d2488.php>>.

³ Physical quantities which transform by $Q\mathbf{U} = \mathbf{u}$ and $QTQ^T = \boldsymbol{\tau}$ will be referred to as vectors and tensors, respectively. Quantities which are merely gathered together to take advantage of Matlab's matrix capabilities will be called arrays.

forward, Y to the left, and Z upward, and let $Q(t)$ be the rotation (special orthogonal⁴) matrix. See Figure 2. Then the rigid-body motion of the vehicle sprung mass is given by

$$\mathbf{x} = Q(t)\mathbf{X} + \mathbf{c}(t), \quad Q(t) \in SO(3),$$

where $\mathbf{c}(t)$ is the motion of the center of mass. Body-fixed vectors \mathbf{U} are transformed into spatial vectors \mathbf{u} via $Q(t)\mathbf{U} = \mathbf{u}$, and vice-versa using $Q^T(t)$: $Q^T(t)\mathbf{u} = \mathbf{U}$. The velocity is given by

$$\mathbf{v} = \dot{Q}(t)\mathbf{X} + \dot{\mathbf{c}}(t), \quad \mathbf{v} = \dot{Q}(t)Q^T(t)(\mathbf{x} - \mathbf{c}(t)) + \dot{\mathbf{c}}(t).$$

The spatial angular velocity tensor is $\hat{\omega}(t) = \dot{Q}(t)Q^T(t)$, while the body-fixed angular velocity tensor is $\hat{\Omega}(t) = Q^T(t)\dot{Q}(t)$. Both $\hat{\omega}$ and $\hat{\Omega}$ are skew-symmetric. These are related to the spatial and body-fixed angular velocity vectors $\boldsymbol{\omega}$ and $\boldsymbol{\Omega}$ via

$$\hat{\omega}\mathbf{u} = \boldsymbol{\omega} \times \mathbf{u}, \quad \hat{\Omega}\mathbf{U} = \boldsymbol{\Omega} \times \mathbf{U}.$$

It is assumed that the wheel centers may only move vertically in the body-fixed frame, corresponding to an ideal suspension constraint. The sprung mass (the vehicle body) interacts with the wheels through suspension forces $\mathbf{P}_k(t)$ (body-fixed) and $\mathbf{p}_k(t) = Q(t)\mathbf{P}_k(t)$ (spatial). (Going forward, a subscript k is implied to run from $1, \dots, 2n$, accounting for the $2n$ wheels.) If the static equilibrium positions of the $2n$ wheel centers in the body-fixed coordinates are \mathbf{R}_k and $\zeta_k(t)$ the vertical suspension displacements, then the spatial positions of the wheel centers are

$$\mathbf{r}_k(t) = Q(t)\{\mathbf{R}_k + \zeta_k(t)\boldsymbol{\partial}_z\} + \mathbf{c}(t).$$

The dynamical equations are Newton's second law for the sprung mass

$$m\ddot{\mathbf{c}}(t) = -mg\boldsymbol{\partial}_z + \sum_{k=1}^{2n} Q(t)\mathbf{P}_k(t) = -mg\boldsymbol{\partial}_z + Q(t) \sum_{k=1}^{2n} \mathbf{P}_k(t),$$

where m is the sprung mass, g is the acceleration due to gravity, and $\boldsymbol{\partial}_z$ is a unit vector pointing vertically, and the moment (Euler) equation for the motion about the center of mass

$$\boldsymbol{\tau}_c(t) \equiv \sum_{k=1}^{2n} (\mathbf{r}_k(t) - \mathbf{c}(t)) \times \mathbf{p}_k(t) - \mathbf{m}_k(t) = \dot{\mathbf{h}}_c(t),$$

where $\boldsymbol{\tau}_c(t)$ is the torque about the center of mass, $\mathbf{r}_k(t)$ are the spatial positions of the wheel centers, $\mathbf{m}_k(t)$ is the spatial moment applied to wheel k , and $\mathbf{h}_c(t)$ is the angular momentum. Transforming to the body-fixed frame we obtain the Euler-Poincaré form

$$\mathbb{I}_c \dot{\boldsymbol{\Omega}}(t) = \mathbf{T}_c(t) - \boldsymbol{\Omega}(t) \times \mathbb{I}_c \boldsymbol{\Omega}(t),$$

where \mathbb{I}_c is the inertia tensor about the center of mass in body-fixed coordinates, $\boldsymbol{\Omega}(t) = Q^T(t)\boldsymbol{\omega}(t)$ is the body-fixed angular velocity vector, $\mathbf{h}_c(t) = Q(t)\mathbf{H}_c(t)$, $\mathbf{H}_c(t) = \mathbb{I}_c \boldsymbol{\Omega}(t)$, and

⁴ The special orthogonal group of matrices in three dimensions $SO(3)$ is the set of matrices satisfying $Q^T Q = I$, $\det Q = +1$.

$\mathbf{T}_c(t) = Q^T(t)\boldsymbol{\tau}_c(t)$ is the body-fixed torque about the center of mass. If $\mathbf{M}_k(t) = Q^T(t)\mathbf{m}_k(t)$ is the body-fixed moment applied to wheel k , it follows that

$$\mathbf{T}_c(t) = \sum_{k=1}^{2n} (\mathbf{R}_k(t) - \zeta_k(t)\boldsymbol{\partial}_z) \times \mathbf{P}_k(t) - \mathbf{M}_k(t) \approx \sum_{k=1}^{2n} \mathbf{R}_k(t) \times \mathbf{P}_k(t) - \mathbf{M}_k(t),$$

if the (assumed small) suspension displacement $\zeta_k(t)$ are ignored.

The terrain height at the positions of the wheel centers are obtained from the OpenCRG⁵ function `crg_eval_xy2z`: $z_k^{CRG} = \text{crg_eval_xy2z}(\mathbf{r}_k)$, $k = 1, \dots, 2n$.

The difference between the wheel center height and the terrain height is used to calculate the deflection δ_k of the each tire (Figure 3) and, assuming a simple linear tire stiffness model, the vertical contact forces on the wheels:

$$\delta_k = \max(0, z_k^{CRG} + R - z_k), \quad F_k^Z = K_k \delta_k, \quad k = 1, \dots, 2n$$

The deflection is limited so that the tire only supports a compressive contact force ($\delta_k \geq 0$).

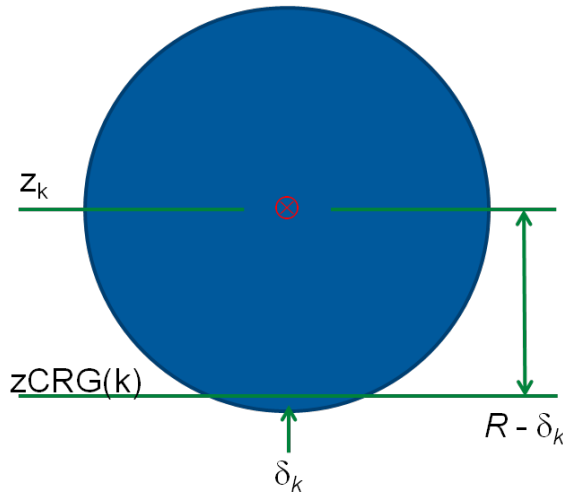


Figure 3. Calculating the tire deflection.

The wheel center velocities and the angular velocities of the wheels are combined to determine the slip velocity. Given a wheel center velocity of \mathbf{v}_k and a rotation speed of $\dot{\rho}_k$ about the body-fixed Y axis (spatial axis $Q(t)\boldsymbol{\partial}_Y$), the velocity \mathbf{v}_k^s of the tire contact patch center at $-RQ(t)\boldsymbol{\partial}_Z$ from the wheel center is

$$\mathbf{v}_k^s = \mathbf{v}_k + (\dot{\rho}_k Q(t)\boldsymbol{\partial}_Y) \times (-RQ(t)\boldsymbol{\partial}_Z) = \mathbf{v}_k - \dot{\rho}_k R Q(t) \boldsymbol{\partial}_X.$$

See Figure 4. In the body-fixed frame this becomes $\mathbf{V}_k^s = \mathbf{V}_k - \dot{\rho}_k R \boldsymbol{\partial}_X$.

⁵ OpenCRG website <<http://www.openerg.org/>>.

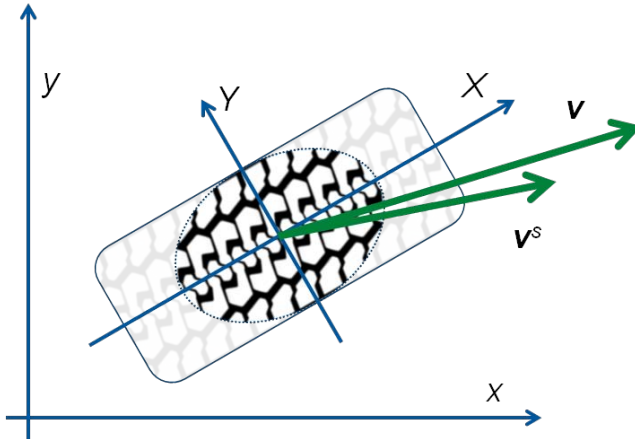


Figure 4. Calculating the slip velocity v^s .

The slip velocity components are thus $V_k^{SX} = V_k^X - \dot{\rho}_k R$ and $V_k^{SY} = V_k^Y$. Therefore the longitudinal slip is $\kappa_k = (\dot{\rho}_k R - V_k^X)/\max(|V_k^X|, |\dot{\rho}_k R|)$, and the slip angle is $\tan \alpha_k = -V_k^Y/V_k^X$. The longitudinal slip definition is modified from most of the references to account for slip without forward motion ($V_k^X = 0$) and locked wheel sliding ($\dot{\rho}_k = 0$); these modified expressions are used in the model. The Pacejka “magic formula” model⁶ uses the normal force, the longitudinal slip, and the slip angle to compute the tire forces and moments.

Once the tire forces and moments are determined, the suspension forces and moments may be approximated, and finally the accelerations of the vehicle body and the wheels may be calculated using the dynamical equations. In order to carry this out a form must be chosen for the rotation matrix; the choice here is $Q = Q_{yaw}(\psi) Q_{pitch}(\theta) Q_{roll}(\phi)$:

$$Q = \begin{bmatrix} \cos \psi \cos \theta & \sin \phi \cos \psi \sin \theta - \cos \phi \sin \psi & \cos \phi \cos \psi \sin \theta + \sin \phi \sin \psi \\ \sin \psi \cos \theta & \sin \phi \sin \psi \sin \theta + \cos \phi \cos \psi & \cos \phi \sin \psi \sin \theta - \sin \phi \cos \psi \\ -\sin \theta & \sin \phi \cos \theta & \cos \phi \cos \theta \end{bmatrix}$$

where the roll, pitch and yaw angles are ϕ , θ , and ψ , respectively.

1.4 Important Findings and Conclusions

The model has been exercised to confirm that the amphibious vehicle can traverse straight, curved, banked and sloped terrain, individually or in combination. Certain limitations of the model have been noted: a tendency to oversteer with the low fidelity tire model and understeer with the Pacejka model. More research into tire models and their interaction with the vehicle dynamics would be advisable. Additionally implementing a fast and accurate tracked vehicle model would be highly useful.

⁶ Egbert Bakker, Lars Nyborg and Hans B. Pacejka, “Tyre modelling for use in vehicle dynamics studies,” SAE Technical Paper 870421, 1987, and H. B. Pacejka, *Tire and Vehicle Dynamics*, Butterworth-Heinemann, first edition 2002, second edition 2006, third edition 2012.

A number of internal variables, such as the tire and suspension forces, the acceleration of the center of mass, etc. should be saved to allow quantitative investigations of the vehicle motion.

1.5 Implications for Further Research

This model would be much more useful with a fast and accurate tracked vehicle option. Further work to make the existing model more robust would also increase its value. Additionally most automotive calculations are done using the SAE J670E surface vehicle standard for coordinate frame and rotation direction definitions; this differs from mine since the SAE J670E y axis is to the right and the z axis is down. Using the SAE J670E standard would make including models from the existing literature easier.